A Model Population-Based Approach to Enhance the Detection of Premature Ventricular Contraction of ECGI

Jorge Sánchez[1], Inés Llorente-Lipe[1], Santiago Ros[2], Felipe Atienza[2,3], Andreu M Climent[1,3], María S Guillem[1,3]

[1] ITACA Institute, Universitat Politècnica de València, Valencia, Spain
[2] Department of Cardiology, Hospital General Gregorio Marañón, Madrid, Spain
[3] Corify Care SL, Madrid, Spain

Abstract

Premature ventricular contractions (PVCs) represent a prevalent cardiac anomaly affecting both individuals with and without structural heart disease, with outflow tract-originated PVCs constituting the majority of idiopathic ventricular arrhythmias. Despite the commonality and potential severity of PVCs, including their role in ventricular fibrillation, accurate diagnosis, and localization remain challenging due to the limitations of traditional 12-lead ECG and the use of rule-based decision algorithms. Electrocardiographic imaging (ECGI) has been introduced as an innovative method to assist in PVC localization, albeit with limitations in pinpointing exact origins. In this study, we explore the power of computer models to create a population database of PVC to refine treatment approaches through an enhanced understanding of electrical propagation dynamics. Through a database of simulated PVCs, we developed a PVC estimation algorithm capable of accurately estimating PVC origins. Our approach offers a promising avenue for personalized and more effective treatment strategies in managing PVC-induced arrhythmias.

1. Introduction

Premature ventricular contractions (PVCs) are common and occur in a broad scope of the population, which includes patients without apparent structural heart disease as well as patients with different cardiac diseases. PVCs originating in the outflow tract can cause ventricular arrhythmias, which are the most common type of idiopathic ventricular arrhythmias, accounting for approximately 70% of cases [1]. However, idiopathic PVCs originating from the left ventricular septum have also been observed [2], and under certain conditions, PVCs may trigger ventricular fibrillation [3].

Currently, PVCs can be diagnosed using the 12-lead ECG [1]. However, the rule-based decision algorithms to locate the PVC origin require accurate measurement of 12-lead ECG intervals and R/S voltage relation, posing challenges for practical and reproducible implementation [1].

The preferred treatment for PVCs is catheter ablation, which creates a non-conducting scar in the tissue from which PVCs arise [4]. Clinically, the precise localization of PVC origins is crucial for determining the most effective ablation strategy. For planning a catheter ablation strategy, the site of origin—whether epicardial or endocardial or located in the right or left ventricle—significantly influences the approach and procedure planning. In recent years, electrocardiographic imaging (ECGI) has emerged as an alternative method to guide ablation treatments. ECGI has been shown to help determine the location of PVCs. Previous work explored the use of ECGI inverse solutions; however, ECGI has limitations in determining the exact location of PVCs located at the septum or the base of the ventricles [5–7].

Several groups have shown the capabilities of computer models to generate realistic potentials at the surface of the torso [8–10]. Thanks to the detailed representation of cardiac electrophysiology, a computer-based population of models can be created to cover the variability that PVCs from different origins can be observed in the body surface potential map (BSPM).

Therefore, in this study, we combine ECGI by using the local activation time (LAT) map with a population-based approach to simulate the PVC propagation that reproduces the potentials at the surface of the torso, offering increased precision in localizing the origin of PVCs compared to ECGI-only estimation. Our proposed approach proved fast enough to be used during clinical practice.

2. Methods

2.1. Model population

We created anatomically detailed meshes derived from non-invasive acquisitions and a statistical shape model.

The torso model and the 128 electrode position were obtained with the Acorys system (Corify Care S.L.) using photogrammetry. The biventricular detailed model of the heart corresponds to the mean shape from the statistical shape model of Rodero et al. [11]. The extracellular medium was considered isotropic, and conductivity for the blood, lung, liver, and torso were 0.7 S/m, 0.0389 S/m, 0.1667 S/m, and 0.8 S/m, respectively [12]. Preferred myocyte orientation was computed using a rule-based method [13]. Additionally, functional regions were added to the ventricular myocardium to set the conduction velocity (CV) to 2.0 m/s for the fast endocardial layer [14] and 0.7 m/s [15] for the mid-myocardium and epicardium with an anisotropy ratio of 3:1. Human cellular ventricular electrophysiology was simulated using the mathematical model proposed by Tomek et al. [16]. The mesh has an average edge length of 350 μm. The bidomain model was solved using openCARP [17] to simulate the electrical propagation at the ventricular myocardium and across the torso.

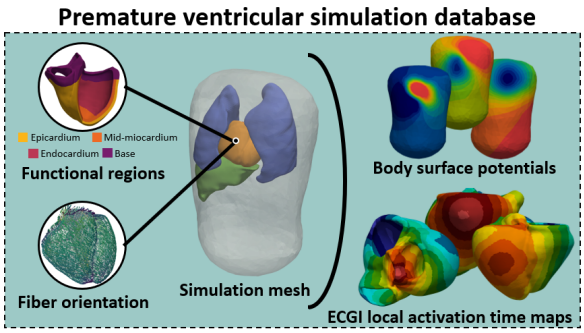

Figure 1. Premature ventricular contraction simulation database. The geometrical model contain heart, liver, lungs, blood and torso. We compute the BSPMs and the ECGI LAT maps.

The total number of simulations that comprise the database is 618 bidomain simulations. In addition, the inverse problem of electrocardiography was solved using an equivalent single layer (ESL) source model and Tikhonov of zero-order regularization to recover the extracellular endocardial and epicardial potential [18]. The L-curve criterion was used to choose the regularization parameter [19]. LAT maps were computed by transforming each reconstructed extracellular potential at the ventricular surface as a sum of sinusoidal wavelets for all the negative slope time samples and amplitude proportional to the slope at that time and selecting the instant of the maximum amplitude of the transformed signal as the instant of activation time [20].

2.2. PVC location algorithm

To enhance the information ECGI provides, the database that consists of 618 bidomain simulations of PVCs was used. Premature beats were distributed at the detailed ventricular geometry using an extended version of the Cobiveco coordinate system [21]. The proposed algorithm starts from the ECGI local activation map and is compared against the database's LAT maps. Then, four database simulations are selected based on the LAT map's highest Pearson's correlation coefficient (CC). Then, the selected models are compared against the BSPMs, and the simulations with a CC higher than 0.7 are used to enter the decision algorithm.

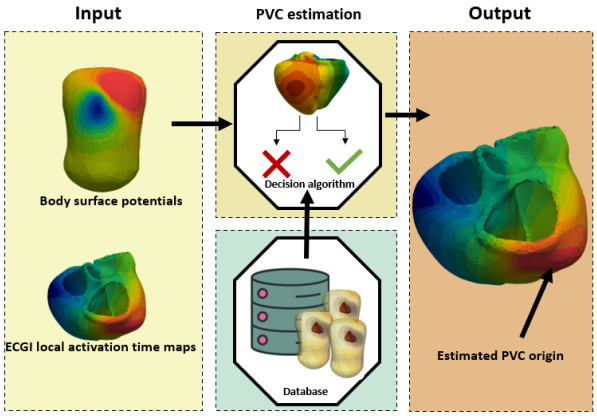

Figure 2. The algorithm's input is the BSPMs and the ECGI LAT map. The PVC estimation is done by comparison with the database and the decision algorithm. As an output, we estimate the PVC origin within the database.

The decision algorithm uses the previously selected simulations and evaluates the transmural coordinates to identify if the PVC comes from the endocardial or epicardial site. Then, the rotational coordinate was evaluated. If the rotational coordinate is between 0.2 and 0.9, the PVC origin is located at the free wall; otherwise, it is at the septum. Then, an extended transversal field added to Cobiveco is evaluated to identify if the origin of the PVC is in the aortic or right ventricular ridge. Then, for the apicobasal coordinate, the median was taken, and for the transventricular coordinate, the mode. The output of the decision algorithm is an extended Cobiveco coordinates for the estimated PVC location.

In addition, the proposed algorithm was evaluated against an independent set of 75 additional bidomain simulations outside the database with a CV of 0.7 m/s. The error of the PVC location was calculated by detecting the earliest activation site in both ECGI and PVC estimation LAT maps. Then, the shortest distance was calculated between the ground truth and ECGI or PVC estimated earli-

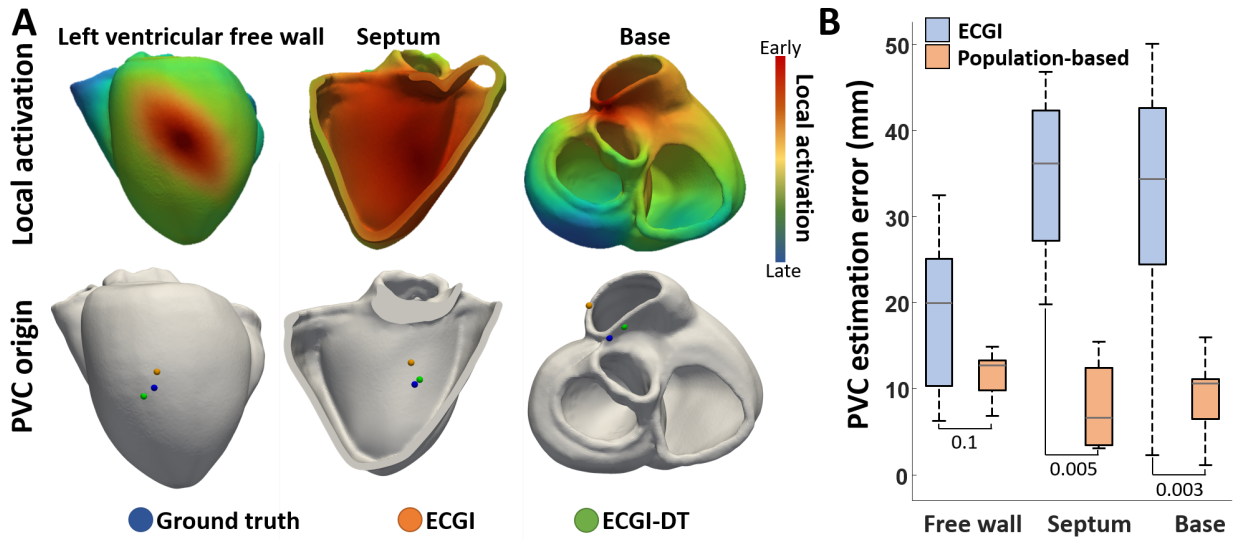

Figure 3. Three examples of PVCs at the free ventricular left wall, septum, and pulmonary outflow tract simulated. A) LAT map and the PVC location (blue) and the estimation with ECGI (orange) and the proposed algorithm (green). B) PVC estimation error of shortest distance of the ventricular free wall, septum, and base.

est activation site. Furthermore, the proposed method will be tested on a patient diagnosed with PVC, where the earliest activation site was determined in the LAT map from intracardiac mapping.

3. Results

The shortest distance error for the earliest activation sites was 33.84±19.23 mm with standard ECGI, but PVC estimation reduced it to 9.28±4.56 mm (Figure 3 panel A) ($p<0.001$). The PVC estimation consistently identified the correct origin chamber (left/right ventricle) and differentiated between endocardium and epicardium origins, unlike standard ECGI (60% chamber, 40% endo/epicardial identification). Our PVC estimation improved the precision of the standard ECGI to localize PVCs in base, septum, and free wall regions (Figure 3 panel B), specifically at the septal and basal regions where standard ECGI was less accurate. Additionally, since the database was pre-computed, the estimation algorithm takes 0.2 minutes to estimate the PVC origin, making it suitable for real-world application in a clinical setup.

Furthermore, the PVC estimation algorithm was tested on a 42-year-old female patient diagnosed with PVC using intracardiac mapping. Standard ECGI estimated the PVC origin at 36.76 mm. In comparison, our estimation based on the population of 618 bidomain simulations gets an error of 15.52 mm measured to the earliest activation site of the LAT map of the endocardial map (Figure 4).

4. Discussion

The proposed PVC estimation improved the location of the origin by decreasing the mean error for different regions of the ventricle (Figure 3 panel B). Additionally, the proposed method takes 0.2 minutes to estimate the location of the PVC, making it suitable for real-world applications in the treatment of PVC. The range of mean error estimation in the literature ranges from 5.0 to 52.2 mm [5–7]. Our PVC estimation achieved a mean error of 9.28±4.56 mm, within the values reported in the literature. Additionally, Duchateau et al. [5], using patient data, reported that in the presence of one epicardial breakthrough, the mean error was 52.2±34.2 mm which agrees with the ECGI values

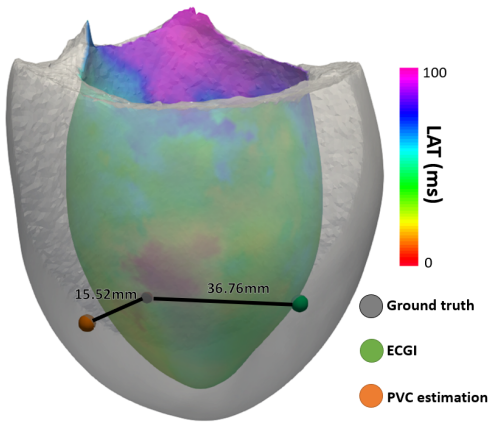

Figure 4. Patient local activation map from endocardial mapping with the earliest activation site (gray circle). The PVC estimated site (orange circle) is close compared to ECGI (green circle) to the PVC.

for the RV and LV free wall of (Figure 3). However, our method improved the location of the PVC in the presence of epicardial breakthroughs compared to standard ECGI (Figure 4).

In conclusion, our approach leverages the power of computational simulations to recreate a population-based algorithm to enhance ECGI capabilities, enabling precise PVC localization even in complex regions such as the septum or the ventricular outflow tracts. Our proposed approach can be used in real-world applications to plan therapeutic approaches to treat PVCs.

Acknowledgments

This project is part of the grant I+D+i PLEC2021-007614, funded by MCIN/AEI/10.13039/501100011033 by RYC2018-024346-I and by CNS2022-135512.

References

[1] Ezzeddine FM, Siontis KC. Localization of outflow ventricular arrhythmias from the electrocardiogram: educated guess, science, or both? Journal of Interventional Cardiac Electrophysiology 6 2023;66:1775–1777. ISSN 1572-8595.

[2] Jia L, Yue-Chun L, Kang-Ting J, et al. Premature ventricular contractions originating from the left ventricular septum: Results of radiofrequency catheter ablation in twenty patients. BMC Cardiovascular Disorders 12 2011;11:27. ISSN 1471-2261.

[3] Sikdar S, Bera D, Kumawat K, et al. An unusual genetic observation in a case of short-coupled pvc-triggered ventricular fibrillation. JACC Case Reports 12 2022;4:101651. ISSN 26660849.

[4] Cronin EM, Bogun FM, Maury P, et al. 2019 hrs/ehra/aphrs/lahrs expert consensus statement on catheter ablation of ventricular arrhythmias. Heart Rhythm 1 2020; 17:e2–e154. ISSN 15475271.

[5] Duchateau J, Potse M, Dubois R. Spatially coherent activation maps for electrocardiographic imaging. IEEE Transactions on Biomedical Engineering 5 2017;64:1149–1156. ISSN 0018-9294.

[6] Dogrusoz YS, Rasoolzadeh N, Ondrusova B, et al. Comparison of dipole-based and potential-based ecgi methods for premature ventricular contraction beat localization with clinical data. Frontiers in Physiology 6 2023;14. ISSN 1664-042X.

[7] Ondrusova B, Tino P, Svehlikova J. A two-step inverse solution for a single dipole cardiac source. Frontiers in Physiology 9 2023;14. ISSN 1664-042X.

[8] Gillette K, Gsell MA, Prassl AJ, et al. A framework for the generation of digital twins of cardiac electrophysiology from clinical 12-leads ecgs. Medical Image Analysis 7 2021;71:102080. ISSN 13618415.

[9] Azzolin L, Eichenlaub M, Nagel C, et al. Personalized ablation vs. conventional ablation strategies to terminate atrial fibrillation and prevent recurrence. EP Europace 2 2023; 25:211–222. ISSN 1099-5129.

[10] Mincholé A, Zacur E, Ariga R, et al. Mri-based computational torso/biventricular multiscale models to investigate the impact of anatomical variability on the ecg qrs complex. Frontiers in Physiology 8 2019;10. ISSN 1664-042X.

[11] Rodero C, Strocchi M, Marciniak M, et al. Linking statistical shape models and simulated function in the healthy adult human heart. PLOS Computational Biology 4 2021; 17:e1008851. ISSN 1553-7358.

[12] Keller DU, Weber FM, Seemann G, Dössel O. Ranking the influence of tissue conductivities on forward-calculated ecgs. IEEE Transactions on Biomedical Engineering 7 2010;57:1568–1576. ISSN 00189294.

[13] Bayer JD, Blake RC, Plank G, Trayanova NA. A novel rule-based algorithm for assigning myocardial fiber orientation to computational heart models. Annals of Biomedical Engineering 10 2012;40:2243–2254. ISSN 0090-6964.

[14] Durrer D, Dam RTV, Freud GE, Janse MJ, Meijler FL, Arzbaecher RC. Total excitation of the isolated human heart. Circulation 6 1970;41:899–912. ISSN 0009-7322.

[15] Taggart P, Sutton PM, Opthof T, et al. Inhomogeneous transmural conduction during early ischaemia in patients with coronary artery disease. Journal of Molecular and Cellular Cardiology 4 2000;32:621–630. ISSN 00222828.

[16] Tomek J, Bueno-Orovio A, Passini E, et al. Development, calibration, and validation of a novel human ventricular myocyte model in health, disease, and drug block. eLife 12 2019;8. ISSN 2050-084X.

[17] Plank G, Loewe A, Neic A, et al. The opencarp simulation environment for cardiac electrophysiology. Computer Methods and Programs in Biomedicine 9 2021;208. ISSN 01692607.

[18] Kalinin A, Potyagaylo D, Kalinin V. Solving the inverse problem of electrocardiography on the endocardium using a single layer source. Frontiers in Physiology 2 2019;10. ISSN 1664-042X.

[19] Hansen PC. The l-curve and its use in the numerical treatment of inverse problems. WIT Press, 2000; .

[20] Hernández-Romero I, Fambuena-Santos C, Herrero-Martin C, Climent AM, Guillem MS. Local conduction velocity estimation during wavefront collisions and reentrant scenarios. In 2022 Computing in Cardiology (CinC), volume 498. 2022; 1–4.

[21] Schuler S, Pilia N, Potyagaylo D, Loewe A. Cobiveco: Consistent biventricular coordinates for precise and intuitive description of position in the heart – with matlab implementation. Medical Image Analysis 12 2021;74:102247. ISSN 13618415.

Address for correspondence:

Jorge Sánchez
ITACA. Ed. 8G-B. Camino de Vera s/n. 46022, Valencia, Spain.
jorsana4@itaca.upv.es